INTERNATIONAL JOURNAL FOR NUMERICAL METHODS IN FLUIDS
Int. J. Numer. Meth. Fluids 2005; **49**:1015–1031
Published online 3 August 2005 in Wiley InterScience (www.interscience.wiley.com). DOI: 10.1002/fld.1040

Assessment of numerical uncertainty for the calculations of turbulent flow over a backward-facing step

Ismail B. Celik*,† and Jun Li‡

Mechanical and Aerospace Engineering Department, West Virginia University, 309 Eng. Sci. Bd., P.O. Box 6106, Morgantown, WV 26506, U.S.A.

SUMMARY

Numerical uncertainty analysis has been performed for the turbulent flow past a backward-facing step. The analysis is based on calculations on seven non-rectangular, but structured, grid sets that were provided by the organizers of the 2004 Lisbon Workshop (*Proceedings of the Workshop on CFD Uncertainty Analysis*, Lisbon, 21–22 October 2004). The calculations were performed by using a commercial code, namely, FLUENT with the Spalart–Allmaras one-equation turbulence model. The present study constitutes a calculation verification process: a set of partial differential equations are solved on gradually refined grid sets, the selected quantities are extrapolated, and then the overall numerical uncertainty in selected quantities is estimated by various methods. Some new ideas are presented for estimating the coefficient of variation, which is related to standard deviation (or standard error of estimate in case of the least squares method).

The major problem that stands out in extrapolation is the cases of non-monotonic convergence. For such cases some alternative methods are proposed, and the results are compared to assess these methods.

KEY WORDS: numerical uncertainty; computational fluid dynamics; flow over a backward-facing step; discretization error; Richardson extrapolation; grid convergence

BACKGROUND

The numerical uncertainty assessment is necessary for computational fluid dynamics (CFD) to become a reliable design tool. Many of the approaches proposed in the literature for quantification of the numerical uncertainty are based on grid refinement in conjunction with Richardson extrapolation (RE) [1–3]. RE usually uses calculations on three grids to determine the extrapolated value of a dependent variable to zero grid size, either using the theoretical order of the scheme (on at least two grid levels), or via the apparent or observed order which

*Correspondence to: Ismail B. Celik, Mechanical and Aerospace Engineering Department, West Virginia University, 309 Eng. Sci. Bd., P.O. Box 6106, Morgantown, WV 26506, U.S.A.
†E-mail: ismail.celik@mail.wvu.edu
‡E-mail: jli1@mix.wvu.edu

Received 30 December 2004
Revised 20 May 2005
Accepted 24 May 2005

is calculated as part of the solution; in the latter case at least three sets of calculations are needed on significantly different grid levels. The pros and cons of this method has been the topic of many recent publications [3–11]. In spite of being a very useful tool for quantifying discretization errors in CFD, there still remain major problems that need to be addressed to advance the level of confidence that could be trusted upon RE [12, 13].

Alternative methods are proposed due to the difficulties of RE. For instance, the least squares approach is proposed [12] to avoid the scattering of the data although it needs more than three grids. The approximate error spline (AES) method [13] is proposed to remedy the non-monotonic convergence problems.

This paper presents our findings from a careful study of numerical uncertainty for one of the test cases proposed by Eça and Hoekstra [14]. This is the classical case of a turbulent flow over a backward-facing step. Our study deals with the following questions: (1) Which extrapolation method is suitable for non-monotonic convergence? (2) Which uncertainty estimation method is a better indicator for grid convergence? (3) How can the error estimates calculated from extrapolated values be translated into a quantitative numerical uncertainty?

METHODS

With four or more grids, we can use the least squares method for extrapolation of computed quantities [12]. With three grids, the following methods: power law method, cubic spline method, polynomial method, and AES method are used in this study (see Appendix A for a brief description of these methods; see also Reference [13] for more details). The linear extrapolation is used for two finest grids. We use the non-linear least squares extrapolation (see Appendix A) with four and seven grids. In these cases the mean, μ, is simply taken as the extrapolated value, ϕ_{ext}. Once ϕ_{ext} is known the numerical uncertainty is calculated using the fine grid convergence index (GCI) proposed by Roache [3] which can be written as

$$\text{GCI} = 1.25 \left| \frac{\phi_{\text{ext}} - \phi_f}{\phi_f} \right| \tag{1}$$

The extrapolated relative error (ERE) can also be used to quantify the uncertainty [6] which is defined as

$$\text{ERE} = \left| \frac{\phi_{\text{ext}} - \phi_f}{\phi_{\text{ext}}} \right| \tag{2}$$

Celik and Karatekin called it ‘the true relative error’, but as a result of communication with Roache [15] we prefer to call it the ‘extrapolated relative error’.

When we apply the least squares method with more than three grids, the scatter in the data indicates a certain amount of uncertainty for the extrapolated value, which could be estimated by calculating the coefficient of variation. In this study, the coefficient of variation (CV) for the least squares method (using at least four grids) is computed from

$$\sigma_r^2 = \sum_{i=1}^{n} [\phi_i - (\phi_{\text{ext}} + \alpha h_i^p)]^2 \tag{3a}$$

$$\sigma_{\phi/h} = \sqrt{\sigma_r^2/n} \tag{3b}$$

$$\mathrm{CV} = \left| \frac{\sigma_{\phi/h}}{\phi_{\mathrm{ext}}} \right| \tag{3c}$$

$$\mathrm{ERE}_{\mathrm{CV1}} = \mathrm{ERE} + \mathrm{CV} \tag{3d}$$

For sufficiently large samples, (3b) should have the factor of $n - n_p$ where $n_p = 3$ (the number of parameters involved in the regression curve). However for small samples, e.g. $n < 10$, this formula has too much bias, hence the factor n in Equation (3b). ϕ_{ext} is equivalent to $\phi(0)$ in Appendix A and it represents the mean in classical statistics notation. σ_r^2 is the sum of the squares of the errors between the non-linear regression curve and the data points. $\sigma_{\phi/h}$ is the standard error of the fit. The CV is the relative error of estimate. $\mathrm{ERE}_{\mathrm{CV1}}$ in Equation (3d) represents the total uncertainty which accounts for both the relative error based on the extrapolated value and the uncertainty induced by the scatter of the data. The GCI already involves a safety factor which should account for the uncertainty in the outcome, hence we did not add CV to GCI, contrary to what has been done by Eça and Hoekstra [16].

For those methods requiring three grids, the CV is calculated from the sampling results with four triplets; Four grids are denoted by G1, G2, G3, and G4, the sample size $n = 4$, and the triplets are (G1,G2,G3); (G1,G3,G4); (G1,G2,G4) and (G2,G3,G4). Using these samples the mean $\overline{\phi_{\mathrm{ext}}}$ is given by

$$\overline{\phi_{\mathrm{ext}}} = \sum_{i=1}^{n} \phi_{\mathrm{ext},i}/n \tag{4a}$$

and the population standard deviation is given by

$$\sigma = \sqrt{\sum_{i=1}^{n} (\phi_{\mathrm{ext},i} - \overline{\phi_{\mathrm{ext}}})^2/(n-1)} \tag{4b}$$

The CV is computed from

$$\mathrm{CV}_{\mathrm{ext}} = \frac{\sigma}{|\overline{\phi_{\mathrm{ext}}}|} \tag{4c}$$

$\mathrm{CV}_{\mathrm{ext}}$ indicates the amount of scatter in the extrapolated values, hence we define

$$\mathrm{ERE}_{\mathrm{CV2}} = \mathrm{ERE} + \mathrm{CV}_{\mathrm{ext}} \tag{4d}$$

Combining different methods of extrapolation, larger samples can be obtained to improve the statistics.

CASE-SPECIFIC ISSUES

The case investigated in this study is a 2D turbulent backward-facing step flow (ERCOFTAC database [17], case 30, see also References [14, 16]). The Reynolds number is 50 000 based on the step height (H) and the maximum inlet velocity. The Expansion ratio is 9/8. Two sets of grids are used for the purpose of this study. The first set has seven grids which are

similar, structured, and non-rectangular grids. The second set has four rectangular grids which are generated by doubling the grid. An example of the first set of grids is shown in Figure 1. These grids are refined from $101*101$ to $241*241$. The maximum $y+$ for the coarsest grid at the south wall is 1.15. The average grid size is calculated from $h=\sqrt{A/n_c}$ where A is the area of the computational domain, and n_c is the number of the cells. The grid refinement ratios for all these grids are in the range of 1.1–1.2 as listed in the first two columns of Table I. These grids are used to estimate the numerical uncertainty with the least squares method. In this study we also selected some triplets to assess those extrapolation methods which are applicable for a set of three grids. For these triplets, the refinement ratios are in the range of 1.29–1.43 which is generally believed to be more appropriate for a grid convergence study with a set of three grids. A set of four grids listed in the last two columns of Table I are also used to estimate the uncertainty with the least squares method and the results are compared to the ones that involved all seven grids.

Spalart–Allmaras' one-equation turbulence model is used to solve for the flow field with the commercial code FLUENT 6.0 [18]. The convection terms and the diffusion terms are discretized with the second-order upwinding scheme and the central differencing scheme, respectively. The inlet velocity is obtained with an empirical multi-layer approach [14, 16, 19]. At the outlet, the gauge pressure and the derivatives of other quantities are set to zero. The no-slip wall boundary condition is used at the walls. If the mesh is fine enough to resolve the laminar sublayer, the shear stress at walls is obtained from laminar stress–strain relationship, i.e. $u/u_\tau=\rho u_\tau y/\mu$. If the mesh is too coarse (i.e. $y+$ is larger than 11), it is assumed that

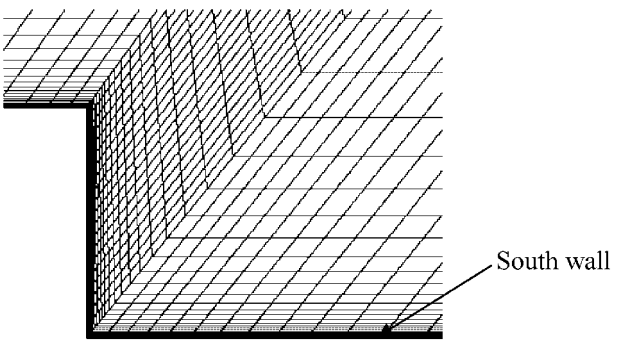

Figure 1. An example of grids used in this study.

Table I. Grid refinement ratios.

Grids	Ratio	Grids	Ratio	Grids	Ratio	Grids	Ratio
$101*101$		$101*101$		$141*141$		$101*101$	
$121*121$	1.20	$141*141$	1.40	$181*181$	1.29	$141*141$	1.40
$141*141$	1.17	$201*201$	1.43	$241*241$	1.33	$181*181$	1.29
$161*161$	1.14					$241*241$	1.33
$181*181$	1.13						
$201*201$	1.11						
$241*241$	1.20						

the centroid of the wall-adjacent cell falls within the logarithmic region of the boundary layer, and the law-of-the-wall is employed, i.e. $u/u_\tau = \ln(E\rho u_\tau y/\mu)/\kappa$, where u is the velocity parallel to the wall, u_τ the shear velocity, y the distance from the wall, κ the von Kármán constant (0.4187), and $E = 9.793$. It should be noted that the first set of seven grids does not require the law of the wall as a boundary condition. Hence we assume none of the grids required the use of the log-law.

All the data shown in this paper are obtained with the second-order upwinding scheme in the solver and the bilinear interpolation method for postprocessing.

Double precision is used for all the calculations so that the round-off errors are expected to be negligible at least for the grid resolution used in this study. The iterations were stopped whenever the scaled residual for continuity equation approached an asymptotic value. The scaled residual is defined as

$$R^\phi = \frac{\sum_{\text{cells}_p} \sum_{nb} |(a_{nb}\phi_{nb} + b - a_p\phi_p)|}{\sum_{\text{cells}_p} |a_p\phi_p|} \tag{5}$$

Here a_p is the centre coefficient of the discretization equation, a_{nb} are the influence coefficients for the neighbouring cells, and b is the contribution of the source term. Correspondingly, ϕ_p is the value for a generic variable at the centre cell and ϕ_{nb} represent the ones at the centre of the neighbouring cells. In this study, the scaled residual is observed to reach a level of about 1E-12–1E-15, which varies with the grids used.

RESULTS AND DISCUSSION

Grid convergence

First the convergence patterns are shown (Figure 2) with grid refinement for the calculated separation point (location where U changes sign from positive to negative) and reattachment point (location where U changes from negative to positive) as well as the velocities at the points $(0, 1.1)$ and $(4, 0.1)$. The separation and reattachment locations were determined using linear interpolation and cubic spline interpolation. The results did not change more than 1%. We also used the criteria of zero shear stress for determining the separation and reattachment points, the results differs less than 0.5% compared to zero velocity results. Two types of grid convergence are identified, namely—monotonic and non-monotonic. We define a convergence is non-monotonic whenever the product $(\phi_i - \phi_{i-1})(\phi_{i+1} - \phi_i)$ is less than zero for any grid index i. It is also seen that the results are far from being grid independent. These figures illustrate that in applications of RE the assumption of being in the asymptotic range is still a problem even with seven grids with reasonable grid refinement at every level.

To emphasize the dependence of grid convergence patterns on the type and the quality of grid distribution we included Figure 3. It is seen that not only the convergence patterns are different but the asymptotic values are too with an uncertainty of about 3.5%. Theoretically, one would expect both have to go to the same extrapolated value as h tends to zero, but this is not the case. However, given that this difference has the same order as the uncertainty calculated in u-velocity at other points (see Tables II, IV and VII) one should not be discouraged too much.

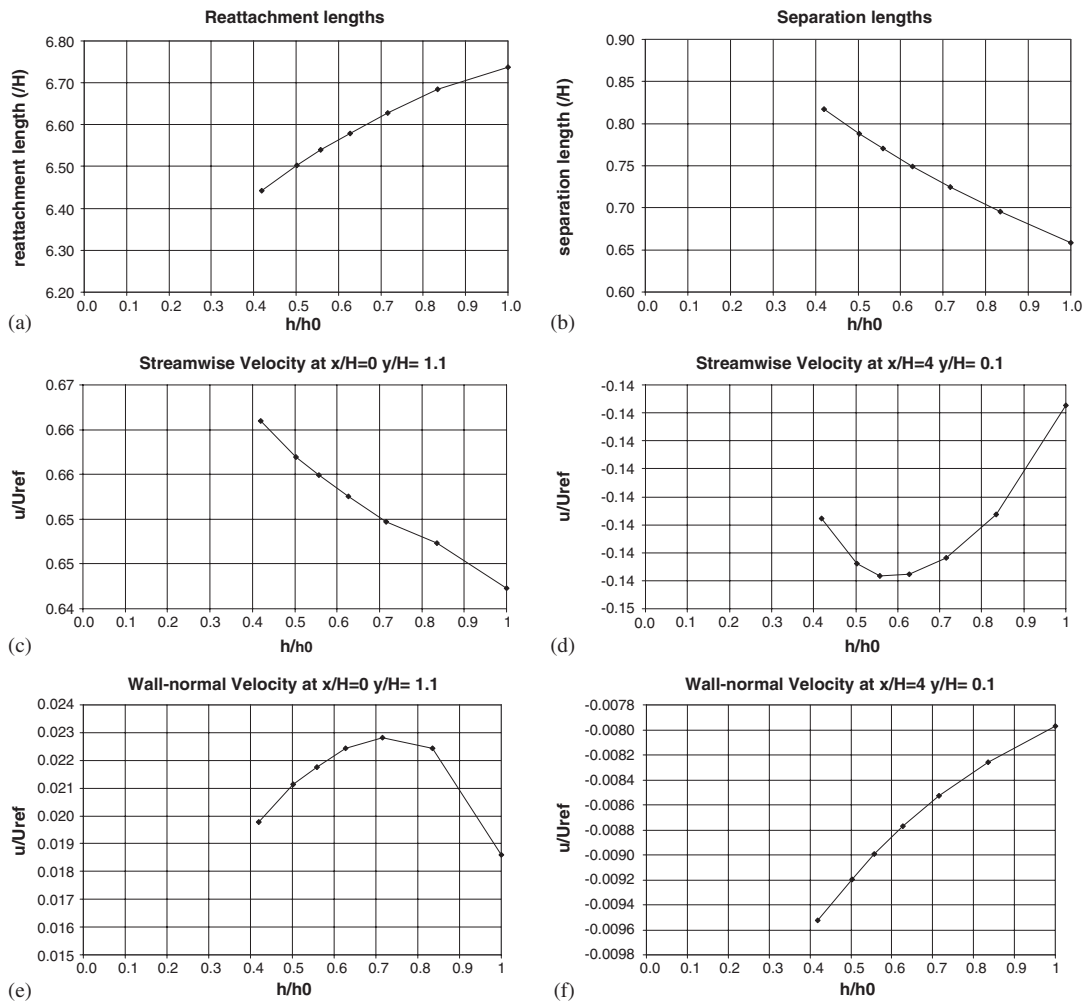

Figure 2. The reattachment and separation lengths, and velocities at $(0, 1.1)$ and $(4, 0.1)$ calculated with different grids (h_0 corresponds to the coarsest grid): (a) 'apparent' monotonic convergence; (b) 'apparent' monotonic convergence; (c) 'apparent' monotonic convergence; (d) non-monotonic convergence; (e) non-monotonic convergence; and (f) 'apparent' monotonic convergence.

Least squares extrapolation

The results in Tables II and III are calculated with the least squares method using all seven grids. Uncertainty is estimated by using the GCI from Equation (1).

The results in Tables IV and V are calculated using the least squares method with four grids: $101 \times 101, 141 \times 141, 181 \times 181, 241 \times 241$. This is done because of two reasons: (1) calculations with seven grids are too expensive; (2) the grid refinement ratio with the set of seven is too small. Here also, uncertainty is estimated by using the GCI.

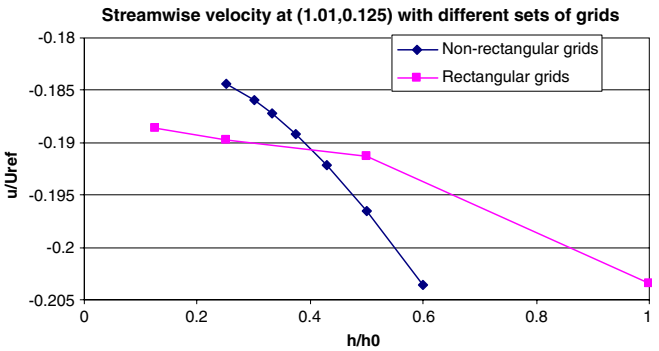

Figure 3. Comparison of rectangular and skewed grid convergence.

Table II. Local flow quantities extrapolated with seven grids.

Variable	$x=0, y=1.1H$	$x=H, y=0.1H$	$x=4H, y=0.1H$
U	6.619E-01	−1.952E-01	−1.442E-01
Uncertainty U	1.7E-03	1.51E-03	2.2E-02
Observed p	1.92	3.00	3.40
V	2.208E-02	1.426E-02	−9.289E-03
Uncertainty V	1.5E-01	7.15E-02	3.1E-02
Observed p	3.23	2.83	3.06
C_p	−1.727E-01	−2.421E-01	−1.164E-01
Uncertainty C_p	1.1E-01	2.26E-03	9.7E-03
Observed p	1.19	2.95	1.33
v_t	1.439E-03	1.192E-03	2.177E-03
Uncertainty v_t	3.9E-04	3.31E-03	4.3E-03
Observed p	3.07	3.06	3.07

Reattachment point: 6.203, uncertainty: 4.6E-2, observed p: 0.86.

Table III. Integral quantities extrapolated with seven grids.

Flow quantity	Predicted	Uncertainty	Observed p
Friction resistance bottom wall (N)	2.640E-02	2.1E-03	3.07
Friction resistance top wall (N)	4.882E-02	2.0E-04	3.06
Pressure resistance bottom wall (N)	1.115E-01	5.6E-03	2.98

The extrapolated quantities and the uncertainties predicted with four grids are very close to the ones predicted with seven grids. Since four grids are the minimum number of grids the least squares approach requires, this seems to be adequate for uncertainty analysis. Of the uncertainties at three different locations $(0,1)$, $(1,0.1)$, and $(4,0.1)$, the ones at $(1,0.1)$ are the largest which may be caused by the rapidly changing flow field in that region. The observed p varies in the range 0.86–3.40. The majority of the cases considered yielded an observed order to be in the range 2.0–3.0 which is encouraging knowing that the nominal theoretical order of the scheme used is 2.0.

Table IV. Local flow quantities extrapolated with four grids.

Variable	$x=0, y=1.1h$	$x=h, y=0.1h$	$x=4h, y=0.1h$
U	6.629E-01	−1.953E-01	−1.439E-01
Uncertainty U	3.5E-03	4.6E-04	1.9E-02
Observed p	1.96	3.14	3.37
V	2.176E-02	1.435E-02	−9.316E-03
Uncertainty V	1.3E-01	6.3E-02	2.7E-02
Observed p	3.21	3.05	3.17
C_p	−1.654E-01	−2.421E-01	−1.196E-01
Uncertainty C_p	5.0E-02	2.3E-03	2.4E-02
Observed p	1.60	3.11	2.59
v_t	1.440E-03	1.193E-03	2.177E-03
Uncertainty v_t	1.2E-03	2.2E-03	4.1E-03
Observed p	3.18	3.18	3.18

Reattachment point: 6.215, uncertainty: 4.4E-2, observed p: 0.89.

Table V. Integral quantities extrapolated with four grids.

Flow quantity	Predicted	Uncertainty	Observed p
Friction resistance bottom wall (N)	2.641E-02	2.0E-03	3.18
Friction resistance top wall (N)	4.883E-02	1.6E-04	3.18
Pressure resistance bottom wall (N)	1.115E-01	5.1E-03	3.12

We also see that some of the variables seem to indicate 'apparent' divergence as the grid is refined (see e.g. Figure 2(b) and (c)), but one has to be cautious to classify these results as 'divergent' for two reasons: (1) in some cases the changes over the span of the scales depicted in the graphs is relatively small, for example, considering the extrapolated value of the reattachment length (Figure 2(a)) be ca. 6.1, there is only 5% error in the finest grid solution; (2) the apparent order of convergence can be $p<1.0$, in which case the derivative as $h\rightarrow 0$ will tend to infinity (if error $\sim ch^p$). One other positive observation is that the least squares method does not lead to unrealistically low (e.g. 0.1) or high (e.g. 10) observed order of accuracy.

Extrapolation with methods using triplets

The quantities extrapolated with power law, AES, cubic spline, and polynomial methods (see Appendix A for explanation of these methods) are compared to those calculated with the least squares method as shown in Table VI. When non-monotonic convergence happens, the extrapolated values predicted with the AES method are closest to the results with the least squares method. The uncertainty indicators GCI, $\mathrm{ERE}_{\mathrm{CV1}}$, and $\mathrm{ERE}_{\mathrm{CV2}}$ are compared in Table VII. It is seen that the uncertainties estimated with GCI and $\mathrm{ERE}_{\mathrm{CV1}}$ using the least squares method is much smaller than the ones by $\mathrm{ERE}_{\mathrm{CV2}}$ using the other methods with only three grids. With the least squares method, the uncertainties based on the $\mathrm{ERE}_{\mathrm{CV1}}$ and $\mathrm{ERE}_{\mathrm{CV2}}$ are consistent with each other, but much larger than the ones with GCI for most cases, which implies that the safety factor of 1.25 in GCI calculation may be too small to represent the uncertainty induced by the scatter of the data. The $\mathrm{ERE}_{\mathrm{CV1}}$ calculated with four

Table VI. Extrapolated quantities with different methods.

		Least squares (7 grids)	Least squares (4 grids)	Power law	AES	Cubic spline	Polynomial
	U	6.619E-01	6.629E-01	6.883E-01	6.586E-01	6.771E-01	6.837E-01
$x=0$	V	2.208E-02	2.176E-02	1.231E-02	2.040E-02	1.533E-02	3.777E-03
$y=1.1$	C_p	−1.727E-01	−1.654E-01	−2.047E-01	−1.515E-01	−1.857E-01	−1.982E-01
	ν_t	1.439E-03	1.440E-03	1.419E-03	1.439E-03	1.428E-03	1.420E-03
	U	−1.952E-01	−1.953E-01	−1.758E-01	−1.965E-01	−1.840E-01	−1.915E-01
$x=1$	V	1.426E-02	1.435E-02	2.301E-02	1.453E-02	1.977E-02	2.231E-02
$y=0.1$	C_p	−2.421E-01	−2.421E-01	−2.273E-01	−2.426E-01	−2.333E-01	−2.352E-01
	ν_t	1.192E-03	1.193E-03	1.065E-03	1.203E-03	1.119E-03	1.174E-03
	U	−1.442E-01	−1.439E-01	−1.379E-01	−1.424E-01	−1.393E-01	−1.265E-01
$x=4$	V	−9.289E-03	−9.316E-03	−1.193E-02	−9.345E-03	−1.094E-02	−1.165E-02
$y=0.1$	C_p	−1.164E-01	−1.196E-01	−1.001E-01	−1.187E-01	−1.071E-01	−9.552E-02
	ν_t	2.177E-03	2.177E-03	2.320E-03	2.176E-03	2.263E-03	2.275E-03
	f(south)	2.640E-02	2.641E-02	2.750E-02	2.638E-02	2.706E-02	2.704E-02
	p(south)	1.115E-01	1.115E-01	9.967E-02	1.118E-01	1.044E-01	1.048E-01
	f(north)	4.882E-02	4.883E-02	4.865E-02	4.884E-02	4.873E-02	4.883E-02
	Reattachment	6.203E+00	6.215E+00	5.992E+00	6.476E+00	6.177E+00	6.054E+00
	Separation	8.988E-01	8.936E-01	1.039E+00	8.018E-01	9.470E-01	9.869E-01

Non-monotonic convergence occurs when refining the grids.

Table VII. Uncertainty of quantities found by extrapolation in Table VI.

		Least square			Linear extrapolation	Power law	AES	Cubic spline	Polynomial
		GCI (7grids)	ERE_{CV1} (7 grids)	ERE_{CV1} (4 grids)	ERE (2 grids)	ERE_{CV2}	ERE_{CV2}	ERE_{CV2}	ERE_{CV2}
	U	1.7E-03	3.4E-03	5.2E-03	3.0E-02	6.0E-02	1.5E-02	2.5E-02	3.9E-02
$x=0$	V	1.5E-01	1.6E-01	1.5E-01	5.2E-01	9.4E-01	1.0E-01	8.1E-01	5.0E+00
$y=1.1$	C_p	1.1E-01	9.9E-02	5.9E-02	1.5E-01	3.4E-01	1.4E-01	1.8E-01	2.3E-01
	ν_t	3.9E-04	4.5E-03	3.8E-03	8.1E-03	3.2E-02	1.3E-02	4.0E-02	5.9E-02
	U	1.5E-03	5.1E-03	4.8E-03	4.6E-02	1.8E-01	4.7E-02	7.4E-02	7.4E-02
$x=1$	V	7.1E-02	1.0E-01	1.0E-01	2.8E-01	5.2E-01	1.9E-01	2.6E-01	3.6E-01
$y=0.1$	C_p	2.3E-03	4.7E-03	5.2E-03	3.3E-02	9.7E-02	2.4E-02	3.7E-02	5.0E-02
	ν_t	3.3E-03	6.8E-03	6.3E-03	5.3E-02	1.9E-01	5.0E-02	9.0E-02	8.0E-02
	U	2.2E-02	2.4E-02	2.3E-02	6.1E-02	6.8E-02	1.7E-02	5.8E-02	1.6E-01
$x=4$	V	3.1E-02	4.6E-02	4.6E-02	1.5E-01	3.1E-01	9.1E-02	1.4E-01	2.0E-01
$y=0.1$	C_p	9.7E-03	2.0E-02	3.5E-02	1.4E-01	2.7E-01	4.2E-02	1.3E-01	2.3E-01
	ν_t	4.3E-03	7.6E-03	8.1E-03	3.2E-02	9.1E-02	2.6E-02	4.1E-02	5.7E-02
	f(south)	2.1E-03	4.1E-03	4.3E-03	2.2E-02	5.9E-02	1.6E-02	2.0E-02	3.3E-02
	p(south)	5.6E-03	1.0E-02	1.1E-02	6.2E-02	1.8E-01	4.1E-02	5.7E-02	9.2E-02
	f(north)	2.0E-04	2.7E-04	2.4E-04	1.9E-03	5.7E-03	1.6E-03	3.8E-03	2.8E-03
	Reattachment	4.6E-02	4.0E-02	3.9E-02	5.0E-02	1.1E-01	2.5E-02	4.7E-02	7.1E-02
	Separation	1.3E-01	9.7E-02	9.3E-02	1.5E-01	3.3E-01	1.0E-01	1.4E-01	2.1E-01

Non-monotonic convergence occurs when refining the grids.

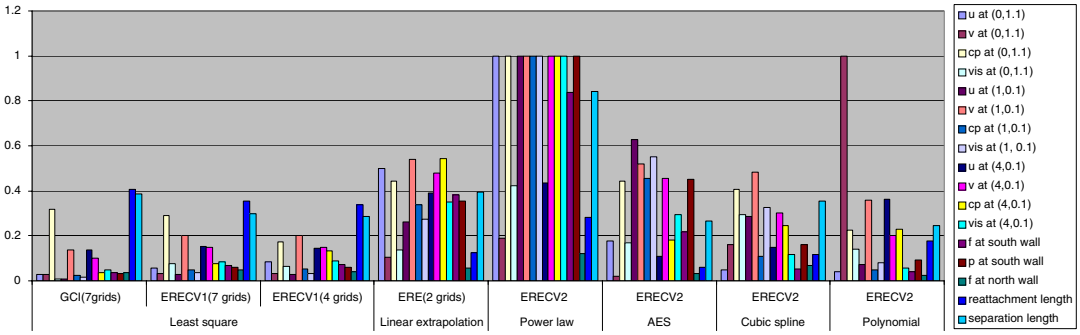

Figure 4. Normalized GCI and ERE_{CV} with different methods and different cases.

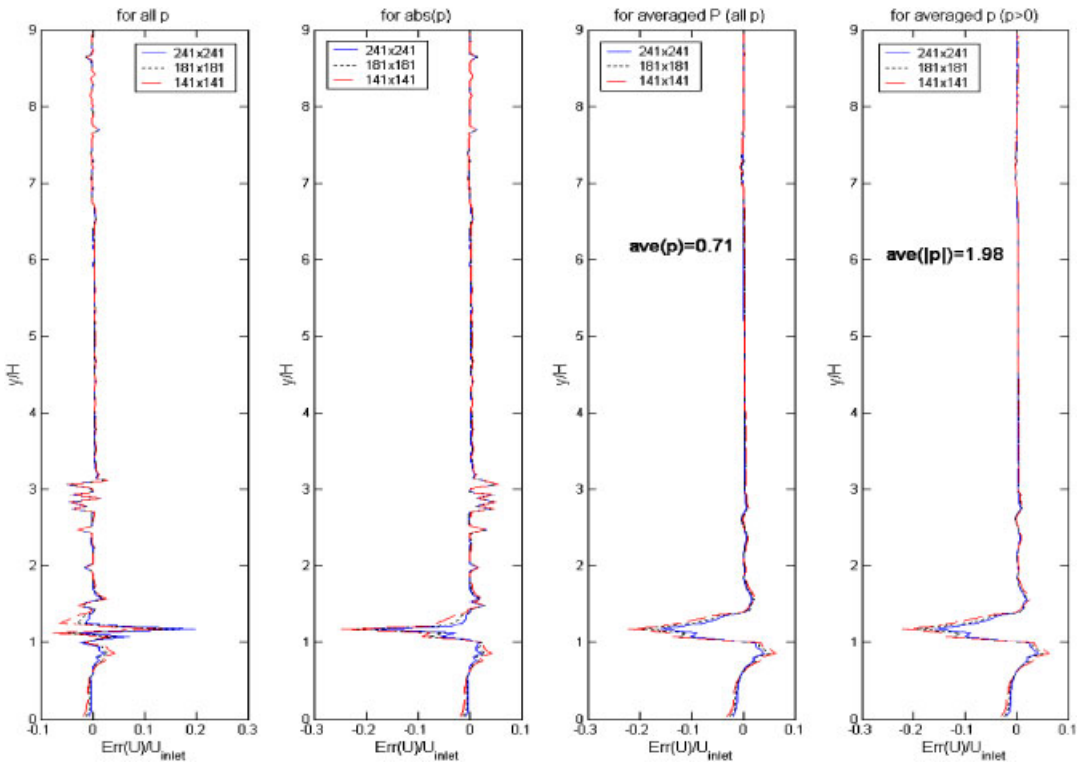

Figure 5. Extrapolated streamwise velocity profile using power law with different ways of utilizing the power p.

grids are larger than the one with seven grids for most cases. The GCI, ERE_{CV1}, and ERE_{CV2} uncertainty measures normalized by the maximum in each row of Table VII are then plotted in Figure 4. Among all the methods applied with triplets, the uncertainty associated with the power law method seems to be much larger than the others and it can be discarded as an outlier. ERE_{CV1} with the least squares method has the same trend as GCI. ERE_{CV2} with AES

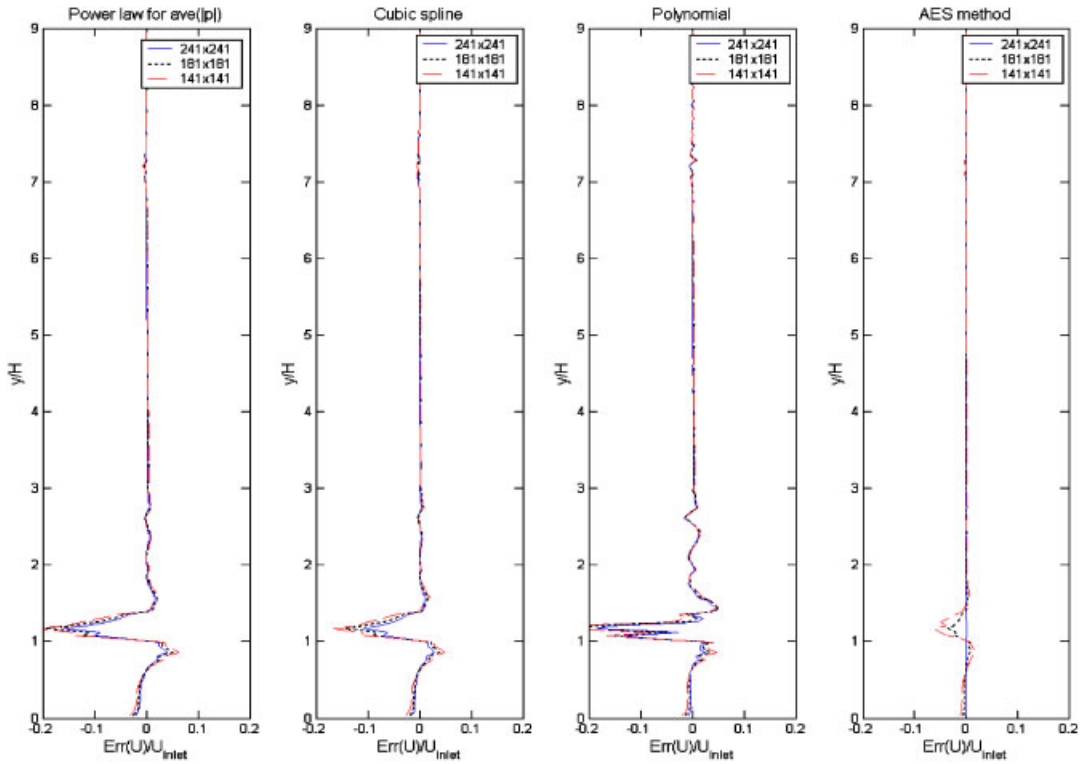

Figure 6. Comparison of the extrapolated streamwise velocity profile at $x/H = 1$ with different methods.

and cubic spline method show similar trends. In most cases, GCI yields the least uncertainty level. It remains to be seen which of these represent the unknown 'reality'. The $\mathrm{ERE}_{\mathrm{CV1}}$ based on the extrapolated value calculated using the least squares method with four grids leads to a much smaller uncertainty than the one that used the linear extrapolation with two finest grids. This is to be expected as first-order approximation should lead to larger uncertainty and can be used if a degree of conservatism is desired.

When reporting results from a CFD application it is usually desirable to present calculated field variables with error bars in terms of profiles at certain locations in parallel with experimental results. Figures 5 and 6 depict the normalized error in the streamwise velocity component at $x/H = 1$ as a function of vertical distance y/H. It is seen that extrapolation using power law is problematic, especially in the region where non-monotonic convergence is present. When an average value is used for the observed order i.e. $p_{\mathrm{ave}} = \sum_{k=1}^{N} p_{k/N}$, N being the number of data points, the results obtained from power law are in concert with the other methods (see Figure 5) where the calculation of p is not an issue. We suspect that the 'reality' is somewhere among the four cases shown in Figure 5. But it remains to be seen which one of these results in Figure 5 indeed represents the 'truth'. This can be clarified by testing these methods against a benchmark with an analytical solution say obtained by the method of manufactured solutions [3]. This is a topic for future study.

Results with no interpolation

In order to eliminate the doubts about interpolation errors, the separation and reattachment lengths calculated with doubling rectangular grids as shown in Table VIII. In this case, the maximum $y+$ for the coarsest grid at the south wall is about 25. Again, a non-monotonic convergence is observed for the reattachment length calculated with rectangular grids. The extrapolated quantities and coefficients of variation are listed in Table IX. For the reattachment length, the uncertainty estimated with the least squares method is the smallest, and for the separation point, the AES method exhibits the smallest uncertainty. The uncertainty in the separation point is large (25–75%), that in the reattachment point is relatively small being in the range of 2–10%.

Comparison of Tables VII and IX show that the extrapolated reattachment length is in general smaller (by about 7%) when the rectangular grids are used with grid doubling.

The streamwise velocity component at $(1.01, 0.125)$ with different grids are shown in Table X. The velocities calculated with the rectangular grids and with no interpolation are shown on the left two columns. On the right, the velocities computed with the non-rectangular grids and with the bilinear interpolation method are shown. The extrapolated values using the least squares method are shown in Table XI. The extrapolated velocity with rectangular grids is somewhat different from the ones with non-rectangular grid. The numerical uncertainty (GCI and $\mathrm{ERE}_{\mathrm{CV1}}$) calculated with the rectangular grids are quite smaller than the ones with the non-rectangular grids. The calculated apparent order of accuracy, p, with rectangular grids is closer to the theoretical order used in this study.

Table VIII. Quantities calculated with Cartesian grids without interpolation.

	$61 * 61$	$121 * 121$	$241 * 241$	$481 * 481$
Separation point	0.0605	0.3143	0.7174	0.8026
Reattachment point	5.5277	5.7498	5.6752	5.8353

Table IX. Extrapolated quantities and coefficients of variation (values in parenthesis are from Tables VI and VII).

	Separation point		Reattachment point	
	Mean	$\mathrm{ERE}_{\mathrm{CV1}}/\mathrm{ERE}_{\mathrm{CV2}}$	Mean	$\mathrm{ERE}_{\mathrm{CV1}}/\mathrm{ERE}_{\mathrm{CV2}}$
Least squares	1.19 (0.89)	3.6E-01 (9.3E-02)	5.77 (6.22)	1.8E-02 (3.9E-02)
Power law	1.39	7.5E-01	5.82	1.0E-01
AES	0.73	2.3E-01	5.75	3.6E-02
Cubic spline	1.00	3.5E-01	5.80	5.6E-02
Polynomial	1.06	5.1E-01	5.80	9.0E-02

Table X. Streamwise velocity at $(1.01, 0.125)$ calculated with different grids.

Rectangular grids	Velocity with no interpolation	Non-rectangular grids	Velocity with interpolation
$61 * 61$	−2.0340E-01	101*101	−2.0360E-01
$121 * 121$	−1.9132E-01	121*121	−1.9647E-01
$241 * 241$	−1.8979E-01	141*141	−1.9210E-01
$481 * 481$	−1.8865E-01	161*161	−1.8916E-01
		181*181	−1.8724E-01
		201*201	−1.8593E-01
		241*241	−1.8433E-01

Table XI. Extrapolated streamwise velocity at $(1.01, 0.125)$ with the least squares method.

	Non-rectangular		Rectangular
	7 grids	4 grids	4 grids
U	−0.1840	−0.1842	−0.1887
GCI	2.0E-03	1.0E-03	2.0E-04
p	3.004	3.146	2.272
ERE_{CV1}	5.6E-03	5.0E-03	2.0E-03

CONCLUSIONS

This extensive effort on analysis of grid convergence and the estimation of numerical uncertainty has shown that when calculations are repeated on significantly different set of four grids, the least squares method gave results that seem to be at least consistent among themselves. We obtained very similar results using seven grids and four grids, hence four sets of carefully selected grids (considering physics of the flow, grid quality and similarity among others) should be adequate for uncertainty analysis. However, application of least squares regression to a set of deterministic calculations may not be easy to justify. One may argue that there are many uncontrollable parameters in a typical CFD application (e.g. local flow regime and scale variations as the grid refined) that may render each simulation essentially a random outcome. The major problem that arises in application of RE again, seems to be with the cases that exhibit non-monotonic convergence. In fact, it may be erroneous to assume monotonic convergence just by observing the behaviour of three or four points. In this regard, it may be necessary to devise methods which perform well both for monotonic, and monotonic cases. Some of the methods that are proposed in this study have shown potential to predict the extrapolated values and the variance for the potentially oscillatory cases without specifically employing the observed order. In particular, the AES method when used with triplets among four grids may be a good choice to estimate the mean extrapolated values and the variance in that mean. The ERE method with four grids originally suggested by Celik and Karatekin [6] when augmented with CV seem to give consistent and similar results as those obtained with seven grids, and reasonable uncertainty levels, in general.

APPENDIX A

Least squares method

With the least squares approach, we compute $\phi_0(\cong \phi_{\text{ext}})$, α, and p by minimizing the following function:

$$\sigma(\phi_0, \alpha, p) = \sqrt{\sum_{i=1}^{n} (\phi_i - \phi_0 - \alpha h_i^p)^2} \tag{A1}$$

where n is the number of grids available. The minimum of (A1) is found by setting the derivatives of (A1) with respect to ϕ_0, α, and p equal to zero, which leads to a non-linear system of equations. Solving the non-linear system yields values for ϕ_0, α, and p.

Polynomial method

This method uses the first few terms in the Taylor expansion of $\phi(h)$ to approximate $\phi(h)$. For instance, assuming the method is first-order, we can use the first three terms if we have a set of three grids. That is

$$\phi(h) = \phi(0) + a_1 h + a_2 h^2 \tag{A2}$$

If we have four grids, we can use

$$\phi(h) = \phi(0) + a_1 h + a_2 h^2 + a_3 h^3 \tag{A3}$$

If the scheme is higher order ($p \geqslant 2$), this method will mean essentially a curve fit to the actual error function. For a fourth-order method one has to keep at least four terms, i.e. five sets of calculations are needed.

The extrapolation to the limit approach is recommended to solve the equations formed by polynomial method. This approach uses the following formula to calculate the extrapolated solution $\phi^{(3)}(h)$ for three grids and $\phi^{(4)}(h)$ for four grids.

$$\phi^{(m)}(h) = \frac{\phi^{(m-1)}(\alpha h) - \alpha^m \phi^{(m-1)}(h)}{1 - \alpha^m}, \quad m = 1, 2, \ldots \tag{A4}$$

It is easy to tabulate the sequential steps of the calculation procedure and to add more points later.

Power law method

We use the power law method proposed by Celik and Karatekin [6] for three grids. The idea follows

$$\phi(0) - \phi(h_1) = c h_1^p \tag{A5}$$

$$\phi(0) - \phi(h_2) = \text{sign}\left(\frac{\varepsilon_{32}}{\varepsilon_{21}}\right) c h_2^p \tag{A6}$$

$$\phi(0) - \phi(h_3) = c h_3^p \tag{A7}$$

where $\varepsilon_{32}/\varepsilon_{32} = (\phi(h_3) - \phi(h_2))/(\phi(h_2) - \phi(h_1))$ the sign of which is positive for monotonic convergence and negative for non-monotonic convergence. There are three unknowns, $\phi(0)$, c, and p. We can implement the same iterative method to solve (A5)–(A7) as done by Celik and Karatekin [6].

For four grids, we can apply

$$\phi(h_i) - \phi(0) = a_1 h_i^p + a_2 h_i^{p+1}, \quad i = 1,2,3,4 \tag{A8}$$

Non-monotonic convergence is facilitated if a_1 and a_2 are of opposite sign. It should be noted that for some cases there is no solution to Equation (A8). Those cases will be counted as unsuccessful outcomes.

Cubic spline method

The well known natural cubic splines curve fitting technique is used to create the cubic splines between three points or four points. $\phi(0)$ can be found by extrapolating the curve for the interval closest to $h = 0$.

AES method

Still using Taylor series expansion for $\phi(h)$ and substituting αh for h, we have

$$\phi(\alpha h) = \phi(0) + a_1 \alpha h + a_2 (\alpha h)^2 + a_3 (\alpha h)^3 + \cdots \tag{A9a}$$

The true error E_t is given by

$$E_t(\alpha, h) \equiv \phi(\alpha h) - \phi(0) = \sum_{k=1}^{\infty} a_k \alpha^k h^k \tag{A9b}$$

and the approximate error E_a

$$E_a(\alpha, h) \equiv \phi(\alpha h) - \phi(h) \tag{A10}$$

where $E_t(\alpha, h)$ is the true error and $E_a(\alpha, h)$ is the approximate error which presents the difference of the subsequent results with the fine grid and the coarse grid. So we have

$$E_a(\alpha, h) = \sum_{k=1}^{\infty} a_k (\alpha^k - 1) h^k \tag{A11}$$

Dividing (A9a) and (A9b) by (A11) and moving $E_a(\alpha, h)$ to the right-hand side yields

$$E_t(\alpha, h) = \frac{1}{1 - (\sum a_k h^k / \sum a_k \alpha^k h^k)} E_a(\alpha, h) \tag{A12}$$

letting

$$\frac{\sum a_k h^k}{\sum a_k \alpha^k h^k} = b_0 + b_1 h + b_2 h^2 \tag{A13}$$

and expanding the l.h.s. of the above equation and comparing it with the r.h.s. gives

$$b_0 = \frac{1}{\alpha}, \quad b_1 = \left(\frac{1-\alpha}{\alpha}\right)\frac{a_2}{a_1}$$
$$b_2 = \left(\frac{1-\alpha^2}{\alpha}\right)\frac{a_3}{a_1} - (1-\alpha)\left(\frac{a_2}{a_1}\right)^2 \tag{A14}$$

Now Equation (A12) can be rewritten as

$$E_t(\alpha, h) = \frac{1}{1-(b_0 + b_1 h + b_2 h^2)} E_a(\alpha, h) \tag{A15}$$

In order to calculate b_0, b_1 and b_2, we need to calculate a_1, a_2 and a_3 first. It is seen from Equation (A11) that

$$a_k = \frac{E_a^{(k)}(\alpha, 0)}{k!(\alpha^k - 1)}, \quad k = 1, 2, 3 \tag{A16}$$

$E^{(k)}$ is the kth derivative of E. Assuming that we have three grids and the solutions as $(h_1, \phi(h_1))$, $(h_2, \phi(h_2))$ and $(h_3, \phi(h_3))$ with $h_3 = \alpha h_2 = \alpha^2 h_1$. And noting that $E_a(\alpha, 0) \equiv 0$ leads to 3 points as $(h_1, E_a(\alpha, h_1))$, $(h_2, E_a(\alpha, h_2))$ and $(0, E_a(\alpha, 0))$ which involves the approximate error instead of the numerical solution $\tilde{\phi}$ itself. Using the information on E_a we can interpolate with cubic splines using two endslopes given by $E_a'(\alpha, 0) \cong 0$ and $E_a'(\alpha, h_1) \cong (E_a(\alpha, h_1) - E_a(\alpha, h_2))/(h_1 - h_2)$. These endslopes are acceptable at $h = 0$ for any scheme with order larger than 1. For the first-order methods, in general, the slope at $h = 0$ is not zero. We could still obtain excellent results using the zero slope assumption for the first-order methods as we demonstrate in the assessment part of this paper. Once we have $E_a^{(k)}(\alpha, 0)$, we can calculate a_k from Equation (A16). As one might notice, b_1 is singular at $h = 0$ if $E_a'(\alpha, 0) = 0$. In order to avoid this singularity, $E_a'(\alpha, \varepsilon)$ can be used to represent $E_a'(\alpha, 0)$ by using finite differencing at $h = \varepsilon$ where ε is a small value. Having obtained b_0, b_1 and b_2, we can calculate $\phi(0)$ from Equation (A15) together with definition (A9a), (A9b) and (A10).

REFERENCES

1. Richardson LF. The approximate arithmetical solution by finite differences of physical problems involving differential equations, with an application to the stresses in a masonry dam. *Transactions of the Royal Society of London, Series A* 1910; **210**:307–357.
2. Richardson LF, Gaunt JA. The deferred approach to the limit. *Philosophical Transactions of the Royal Society of London, Series A* 1927; **226**:299–361.
3. Roache PJ. *Verification and Validation in Computational Science and Engineering*. Hermosa Publisher: Albuquerque, 1998.
4. Celik I, Chen CJ, Roache PJ, Scheurer G (eds). Quantification of uncertainty in computational fluid dynamics. *ASME Publ. No. FED-Vol. 158*, ASME Fluids Engineering Division Summer Meeting, Washington, DC, 20–24 June, 1993.
5. Celik I, Zhang WM. Application of Richardson extrapolation to some simple turbulent flow calculations. In *Proceedings of the Symposium on 'Quantification of Uncertainty in Computational Fluid Dynamics'*, Celik I *et al.* (eds), ASME Fluids Engineering Division Summer Meeting, Washington, DC, 20–24 June, 1993; 29–38.
6. Celik I, Karatekin O. Numerical experiments on application of Richardson extrapolation with nonuniform grids. *ASME Journal of Fluids Engineering* 1997; **119**:584–590.
7. Roache PJ. Quantification of uncertainty in computational fluid dynamics. *Annual Review of Fluid Mechanics* 1997; **29**:123–160.

8. Roache PJ. Conservatism of the GCI in finite volume computations on steady state fluid flow and heat transfer. *ASME Journal of Fluids Engineering* 2003; **125**:731–732.
9. Stern F, Wilson RV, Coleman HW, Paterson EG. Comprehensive approach to verification and validation of CFD simulations—Part 1: methodology and procedures. *ASME Journal of Fluids Engineering* 2001; **123**: 793–802.
10. Cadafalch J, Perez-Segarra CD, Consul R, Oliva A. Verification of finite volume computations on steady-state fluid flow and heat transfer. *ASME Journal of Fluids Engineering* 2002; **124**:11–21.
11. Eça L, Hoekstra M. An evaluation of verification procedures for CFD applications. *24th Symposium on Naval Hydrodynamics*, Fukuoka, Japan, 8–13 July, 2002.
12. Eça L, Hoekstra M. Uncertainty estimation: a grand challenge for numerical ship hydrodynamics. *6th Numerical Towing Tank Symposium*, Rome, September 2003.
13. Celik I, Li J, Hu G, Shaffer C. Limitations of Richardson extrapolation and possible remedies for estimation of discretization error. *Proceedings of HT-FED2004*, ASME Heat Transfer/Fluids Engineering Summer Conference, Charlotte, North Carolina, U.S.A., 11–15 July, 2004, HT-FED2004-56035.
14. Eça L, Hoekstra M (eds). *Proceedings of the Workshop on CFD Uncertainty Analysis*, Lisbon, 21–22 October, 2004.
15. Roache PJ. Personal Communication, 2001.
16. Eça L, Hoekstra M. On the grid sensitivity of the wall boundary condition of the k–ω turbulence model. *ASME Journal of Fluids Engineering* 2004; **126**:900–910.
17. ERCOFTAC Classic Collection Database—http://cfd.me.umist.ac.uk/ercoftac, accessed on 11 December 2005.
18. FLUENT company. *FLUENT 6.0 User Reference Manual*, 2004.
19. Driver DM, Seegmiller HL. Features of a reattaching turbulent shear layer in divergent channel flow. *AIAA Journal* 1985; **23**(2):163–171.
20. Phillips GM, Taylor PJ. *Theory and Applications of Numerical Analysis*. Academic Press: London, New York, 1973; 345.
21. Spalart PR, Allmaras SR. A One-equations turbulence model for aerodynamic flows. *AIAA 30th Aerospace Sciences Meeting*, Reno, January 1992.

